歩行障害

金丸 和富

東京都老人医療センター神経内科医長

はじめに

歩行が円滑に行われるためには、筋力や平衡機能、骨・関節運動などの運動系、四肢や体幹の位置などの情報を伝達する深部覚や視覚、聴覚などの感覚系、周囲の状況に対する反応性、自分の運動能力や周りの状況、位置などを総合的に判断する認知機能、歩行可能な心肺機能などの様々な機能、および、歩行能力に合った環境が必要である[1]。高齢者においては、多くの因子が重なって歩行障害を生じやすい。歩行障害の原因を検討し、治療やケアの方針をより明確にすることは、ADLの維持や転倒防止の点から重要となる。

歩行障害をきたす原因疾患

高齢者において歩行障害や転倒をきたす要因は、図1に示すように多数ある。

1．脳血管障害

脳血管障害により、片麻痺や運動失調、感覚障害を生じると歩行が困難になる。脳梗塞(脳血栓、脳塞栓)や脳出血、くも膜下出血が多い。

脳梗塞は発症機序により、血栓性、塞栓性、血行力学性に分類される。脳内の血管が動脈硬化を基盤に血栓でつまるものが脳血栓で、血栓が脳以外から血流を介して運ばれ脳の血管をつまらせるものが脳塞栓である。脳血栓は、アテローム型脳血栓とラクナ梗塞に大別される。アテローム型脳血栓は、内頸動脈から脳主幹動脈のアテローム性動脈硬化を基盤として、さらに血栓ができ閉塞することによって発症する脳梗塞をさす。高血圧とともに糖尿病や高脂血症との関連が大きい。ラクナ梗塞は、大脳深部(基底核や視床、大脳白質)や脳幹にみられる穿通枝の小梗塞(15mm径以下)をいう。主に高血圧が関与している。

脳内出血の大部分は、高血圧性脳出血である。脳内の細動脈が動脈硬化でもろくなり破れて出血する。好発部位としては、被殻、視床、小脳、脳幹がある。その他の原因としては、脳動静脈奇形やもやもや病がある。また、高齢者においては、脳のアミロイド・アンギオパチーを原因とする皮質下出血が多い。この場合、通常の高血圧性脳出血とは異なり、大脳皮質近くに出血が起こる。くも膜下出血には外傷性と非外傷性のものがあるが、非外傷性のほとんどは脳動脈瘤の破裂によるものである。

最近の動向としては、高血圧に関連した脳出血やラクナ梗塞が減少しているものの、肥満や耐糖能異常、高脂血症といった代謝異常に関連したアテローム型脳血栓や高齢化に伴い心房細動による脳塞栓が増加している。診断は、臨床症状や頭部CT、MRI

1 加齢
2 神経疾患や心血管系疾患、整形外科的疾患
（脳卒中後遺症、パーキンソン症候群、起立性低血圧、変形性脊椎症など）
3 精神疾患
（痴呆やうつ）
4 社会的・環境的要因
（独居、段差のある床など）
5 薬剤
（睡眠剤、安定剤、降圧薬など）
6 特殊な行動
（入浴や排泄など）
7 転倒の既往

図1 歩行障害や転倒の要因

［文献2）より引用］

によって行う。

発症早期から運動療法を行い、必要に応じて装具を作成する。また、再発予防のために、高血圧や糖尿病など脳血管障害の危険因子の治療や抗血小板剤（アスピリンなど）、あるいは、抗凝固剤（ワルファリン）を用いた薬物治療を行う。

頭部CTやMRIにおいて明らかな脳血管障害を認めなくても、内頸動脈狭窄などに起因する一過性脳虚血発作（TIA）や椎骨脳底動脈循環不全によって歩行障害をきたす場合がある。

2．パーキンソン病

振戦、筋強剛（固縮）、寡動・無動、姿勢反射の障害がパーキンソン病の4大症候である。中脳の黒質や大脳基底核を総称して錐体外路系と総称しており、錐体外路症状ともいう。一側上肢の振戦で初発することが多いが、高齢になるとその頻度は低下し、筋強剛や歩行障害で初発することが多くなる。歩行障害の特徴としては、歩幅が小さく小刻み歩行（小歩症）となり、前傾姿態で手の振りが少ない。症状が進行すると姿勢反射の障害が起こり、バランス不良となって転倒しやすくなる。歩き始めや方向転換時に足が前に出ない「すくみ足」も出現することがある。

診断は、まず臨床症状から疑うが、鑑別として、薬剤性パーキンソニズム（スルピリド、ハロペリドールなどによる）、進行性核上性麻痺や線条体黒質変性症などの変性疾患、血管性パーキンソニズム（脳血管障害によるパーキンソン症状）、正常圧水頭症などを除外する必要がある。特に、進行性核上性麻痺は、転びやすい症状（易転倒）が早期から出現するので注意を要する。

治療は、薬物治療が中心となる。ドパミンを補充する目的でのL-ドパ剤とドパミン受容体刺激薬（ドパミンアゴニスト）を中心に用いる。その他、薬物治療では不十分な場合、外科的治療（視床中間質外側核の破壊術や深部電極による持続的刺激）の適応となる。

3．末梢神経障害（ニューロパチー）

四肢末梢神経の障害によって起こる。末梢神経には運動、感覚、自律神経があり、それぞれの障害の程度に応じて症状が出現する。病変の分布より、単ニューロパチー、多発単ニューロパチー、多発ニューロパチーに分類される。

単ニューロパチーは、圧迫性ニューロパチーが主であり、歩行障害をきたすものとしては、腓骨骨頭

部圧迫による腓骨神経麻痺がある。

多発単ニューロパチーには、結節性多発動脈炎(periarteritis nodosa：PN)によるニューロパチーがある。複数の末梢神経が障害されるが、非対称性である。

多発ニューロパチーは、四肢末端の筋力低下、感覚障害(手袋・靴下型)を呈する。左右対称性に四肢遠位部が障害される。原因は多岐にわたり原因検索が治療方針決定のうえで重要となる。特に、糖尿病性、抗癌剤などによる薬剤性、あるいはアルコール性(あるいはビタミン欠乏性)ニューロパチーの頻度が高い。その他、n-ヘキサン(シンナー)などによる中毒性、免疫異常に伴うもの、悪性腫瘍に伴うものがある。

4．整形外科的疾患：変形性脊椎症・膝関節症

脊椎の変形による、脊髄の圧迫(脊髄症)や神経根の圧迫により歩行障害をきたす。症状は慢性に経過するが、転倒により急激に悪化することがある。頸椎症性脊髄症によるバランス障害により転倒しやすくなる場合がある。

間欠性跛行は、一定の距離を歩くと歩行が困難となりしばらく休むとまた歩ける状態をさす。閉塞性動脈硬化症などによって起こる血管性のものと、腰椎脊椎間狭窄症によって起こる神経性のものに大別される。

膝関節軟骨の退行性変性疾患である変形性膝関節症は、加齢とともに急増する。主症状は、歩行時の疼痛であり、治療としては、非ステロイド性消炎鎮痛薬などによる薬物療法、温熱や電気などの物理療法、筋力強化訓練などの運動療法、足底板などの装具療法、人工関節置換術などの外科的療法がある。

5．心血管系

不整脈や起立性低血圧によるめまいやふらつき、閉塞性動脈硬化症などによる下肢循環障害によって歩行障害をきたす。

6．耳鼻科・眼科的疾患

内耳障害によるめまい(良性発作性頭位変換性めまい)や眼科疾患(白内障や緑内障など)による視力障害によって歩行障害をきたす。

7．認知症・うつ病

アルツハイマー病や血管性痴呆、パーキンソン病に伴う痴呆、うつなども歩行障害や転倒のリスクとなる。

転倒防止への対策

高齢者の転倒は、患者側の因子(心身機能の低下)や外的・環境因子など多数の要因が相互に関連して発生する(図1)。多方面からのリスクを検討し転倒の予防対策を立てることが重要となる[2)]。

1．疾患の診断と治療

前述した歩行障害をきたす疾患について診断し、それぞれの治療方針をたてる。その他、認知機能や一般的な内科疾患の有無、健康状態、栄養状態のチェックも必要となる。

2．転倒に関連する薬物の注意

転倒の要因になりやすい薬物の使用について注意する。

①安定剤や睡眠薬

安定剤や睡眠薬は、ふらつきやバランス障害をきたしやすいので、不必要な投与、過度の投与は避ける。特に、認知障害のある患者や歩行障害をきたす基礎疾患を有する患者は要注意である。

②降圧薬

過度の降圧は、めまいやふらつきの原因となるので注意する。

③糖尿病治療薬

糖尿病治療薬の過量投与による低血糖は、ふらつきや転倒の原因となるので注意する。

④パーキンソニズムを生じる薬剤

パーキンソン症状は歩行障害やADLの低下に直結するので、その原因となる薬物の使用は、特に高齢者において注意が必要である。その主な薬剤としては、スルピリド、ハロペリドールなどがある。

3．転倒に関する指導

①転倒防止の重要性(転倒がADLの低下や寝たきり状態、死亡につながること)を十分説明する。
②転倒が起こりやすい状況、場所、時間を指導する。
③転倒の既往、その状況について調査する。
④常に適切な運動を心がけ運動能力を維持する。
⑤過度な説明により、不安や恐怖心を与えすぎないよう注意する。

4．環境の整備

①つまずきがないように段差をなくす。
②滑りにくい床にする。敷物が動かないようにする。
③床に障害物を置かない。
④照明は十分明るさを保つようにする。
⑤家具はよりかかっても倒れないように安定させる。
⑥階段やトイレ、浴室、廊下などに手すりをつける。

References

1) 森　茂美：ヒトの直立二足歩行のメカニズムと加齢変化．*Geriat Med* **43**：7-14、2005
2) 新野直明：転倒リスクの多因子評価．*Geriat Med* **43**：61-65、2005

Acta Oto-Laryngologica, 2005; 125: 1351–1355

Taylor & Francis
Taylor & Francis Group

CASE REPORT

Magnetoencephalography and positron emission tomography studies of a patient with auditory agnosia caused by bilateral lesions confined to the auditory radiations

KIMITAKA KAGA[1], TAKAHIDE KURAUCHI[1], MASAKO NAKAMURA[1], MITSUKO SHINDO[2] & KENJI ISHII[3]

[1]*Department of Otolaryngology, University of Tokyo,* [2]*Department of Language Disorders, Sophia University and* [3]*Department of Positron Research, Geriatrics Research Institute of Tokyo, Tokyo, Japan*

Abstract

The aim of this study was to investigate auditory cortex function in the context of auditory stimuli in a patient with auditory agnosia due to bilateral lesions confined to the auditory radiations. A male patient experienced mild left temporal hemiplegia because of right putaminal hemorrhage at the age of 43 years. Thereafter he recovered completely but hypertension persisted. When he was 53 years old, he suffered left putaminal hemorrhage and went into a coma. After recovering from the coma and right hemiplegia he could hear but could not discriminate speech sounds. Brain CT and MRI demonstrated small bilateral lesions confined to the auditory radiations. Magnetoencephalography demonstrated the disappearance of middle latency responses and auditory-evoked potential studies showed a very small Pa peak. In contrast, a positron emission tomography study demonstrated a marked increase in blood flow in the bilateral auditory cortex in response to both click and monosyllable stimuli. It is speculated that the auditory cortex receives functional projections from the cochlea via non-specific pathways in the cerebral hemispheres.

Keywords: *Auditory agnosia, auditory radiation, magnetoencephalography, positron emission tomography*

Introduction

Auditory agnosia is caused by bilateral lesions in the auditory cortex, auditory radiation or medial geniculate body [1–4]. However, in the case of bilateral lesions involving only the auditory radiations, it is not known what function remains in the preserved but isolated auditory cortex.

There are two parallel auditory systems in the brain [5]. The most important is the primary auditory pathway, which conveys neural signals of speech, music and environmental sounds from the cochlea through the cochlear nerve, brainstem auditory pathway and medial geniculate to the auditory radiation and auditory cortex. The other system is the non-specific auditory pathway, which conveys neural signals from the cochlea through the pontine and thalamic reticular formation or medical geniculate body to the cerebral cortex.

The aim of this study was to investigate whether function is absent or present in the auditory cortex of a patient with auditory agnosia due to bilateral lesions of auditory radiations but with a preserved auditory cortex. The investigation was conducted using magnetoencephalography (MEG), auditory-evoked potential (AEP) studies and position emission tomography (PET). Many MEG studies of auditory cortex function have been reported [6–9] but studies of patients with auditory cortex lesions are rarely reported [10].

Case report

A male patient experienced left mild temporal hemiplegia as a result of right putaminal hemorrhage at the age of 43 years. Thereafter he recovered completely but hypertension persisted. When he was 53 years old, he went into a coma due to left

Correspondence: Kimitaka Kaga, Department of Otolaryngology, Faculty of Medicine, University of Tokyo, 7-3-1 Hongo, Bunkyo-ku, Tokyo, Japan. Tel: +81 3 5800 8665. Fax: +81 3 3814 9486. E-mail: kimikaga-tky@umin.ac.jp

(Received 4 November 2004; accepted 4 November 2004)

ISSN 0001-6489 print/ISSN 1651-2551 online
DOI: 10.1080/00016480510027501

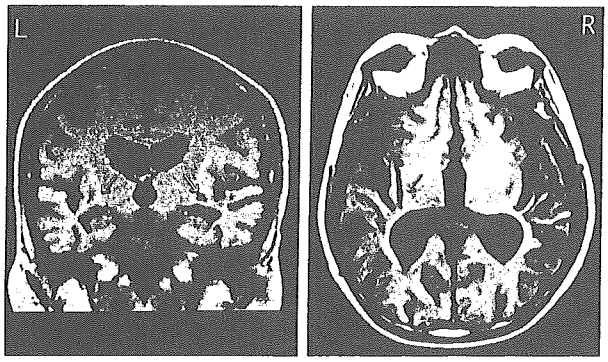

Figure 1. Brain MRI scan. In both hemispheres, the auditory radiations are damaged (*arrows*) by small brain infarctions.

putaminal hemorrhage. After recovering from the coma, he manifested mild right hemiplegia and hearing problems. The hemiplegia resolved with the exception of some residual weakness, but the auditory problems persisted. Although the patient could hear, he could not discriminate any speech, music or environmental sounds. Brain CT and MRI demonstrated localized small lesions in the bilateral auditory radiation only (Figure 1). Pure-tone audiometry revealed bilateral mild hearing loss (Figure 2).

AEP studies (Figure 3) demonstrated a normal electrocochleogram (EcochG), auditory brainstem response (ABR) and middle latency response (MLR). The K complex to sound stimuli was clearly recorded on electroencephalography (EEG) (Figure 4).

Neuropsychological tests demonstrated that although the patient could not discriminate any speech, music or environmental sounds he did not have aphasia (Figure 5). He was diagnosed as having auditory agnosia due to bilateral lesions confined to the auditory radiation, with preservation and isolation of the auditory cortex bilaterally. Subsequently, his pure-tone threshold worsened in the higher frequencies (Figure 2).

MEG, AEP and PET studies

Audiological and neuropsychological tests were conducted to investigate the patient's auditory function and perception. Thirty-two-channel MEG was used to study middle latency auditory-evoked magnetic fields (MLAEFs), while electrical middle latency responses (EMLRs) were simultaneously recorded for comparison [5]. PET using fluorodeoxyglucose was conducted to investigate blood flow in the auditory cortex in response to auditory stimuli, consisting of clicks and monosyllables.

MEG and AEP studies were conducted 4 years after the second hemorrhage, at the time of the second audiogram shown in Figure 2. They demonstrated that MLAEFs were absent, with a very small Pa peak in the EMLR (Figure 6). In contrast, the PET study demonstrated increased blood flow in the bilateral auditory cortex in response to clicks and Japanese monosyllable verbal stimuli (Japanese monosyllables generally correspond to consonant–vowel sounds in English). Cerebral blood flow increased by at least 10% above the resting baseline in areas of the auditory cortex, especially with verbal stimuli, but did not reach the 20% increases typical of normal subjects (Figure 7).

Discussion

In this patient, the results of audiological and neuropsychological examinations were almost the same as those in patients with auditory agnosia or cortical deafness, which are caused by bilateral lesions of the auditory cortex [2,3]. However, because the auditory cortex was not damaged in

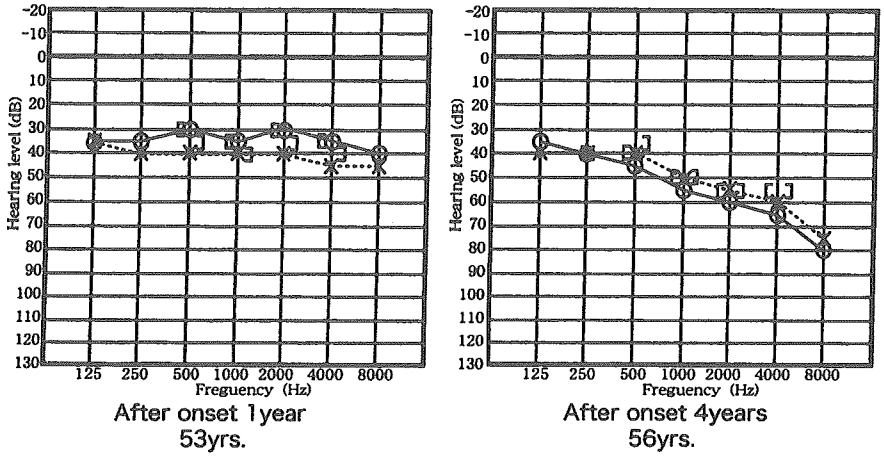

Figure 2. Pure-tone audiograms recorded 1 and 4 years after the second hemorrhage. The tests reported here were performed at the time of the later audiogram.

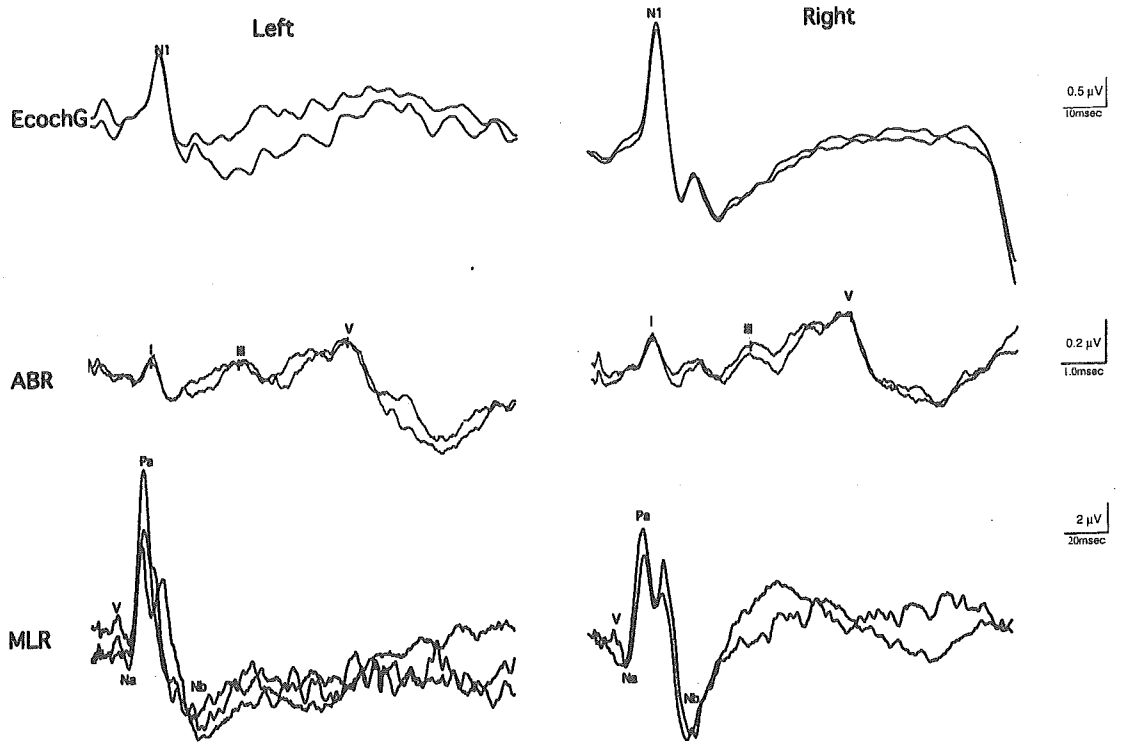

Figure 3. Results of the AEP studies. EcochG, ABR and MLR were normal in the right and left ears.

our patient, our concern was to investigate, using objective measures, whether the auditory cortex could respond to auditory stimuli.

There are two auditory pathways in the brain [5,11,12]. The most important is the specific auditory pathway, which is used for auditory perception. The other is the non-specific auditory pathway, which is involved in arousal [5,12]. Although our patient's specific auditory pathway was damaged at the subcortical level of the auditory radiation, the non-specific auditory pathway was preserved. The PET study demonstrated an increase in blood flow in the auditory cortex of 10% (approximately half of normal) in response to auditory stimuli. However,

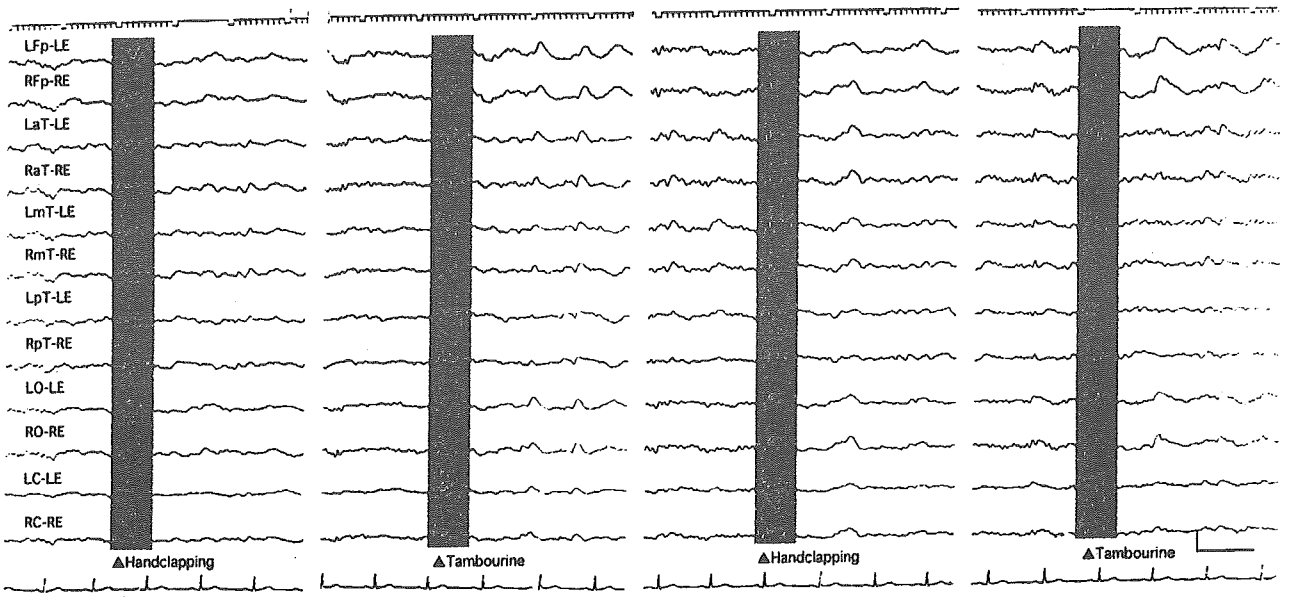

Figure 4. EEG recording. The K complex to sound stimuli was recorded from all electrode leads (shadow area).

(a) Speech Audiometry

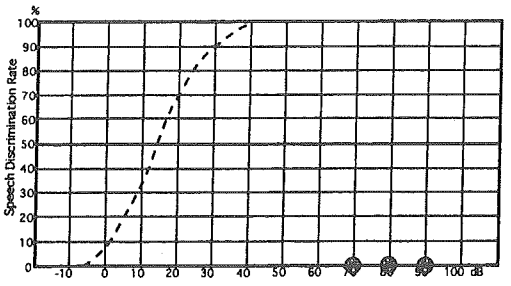

(b) Enviromental sound perception test

Test Sound		Response	
		Oral Answer	Picture Matching
Human	1. Man's voice	×	×
	2. Woman's voice	×	×
	3. Singing	×	×
	4. Baby's cry	×	○
	5. English speech	×	×
	6. Laughter	×	○
Animal and Bird	1. Mewing(cat)	×	○
	2. Barking (dog)	○	○
	3. Mooing (cow)	×	×
	4. Neighing (horse)	×	×
	5. Cawing (crow)	×	○
	6. Crowing (cock)	×	×
Instrument	1. Drum	○	○
	2. Trumpet	×	○
	3. Wall clock	×	○
	4. Telephone ring	×	×
Nature	1. Whistle of wind	×	×
	2. Wave	×	○
	3. Stream	×	×
Artificial	1. Electric train	×	○
	2. Car	×	×
	3. Gunshot	○	×
	4. Saw	×	×
	5. Footsteps	×	×
		12.5%	41.5%

Figure 5. Results of the auditory perception tests. (a) Speech audiometry demonstrated zero discrimination at any intensity. (b) The environmental sound perception test showed poor performance as well (circles indicate correct responses). Normal individuals typically score 100% on both the open-set oral responses and the much less difficult closed-set picture matching task.

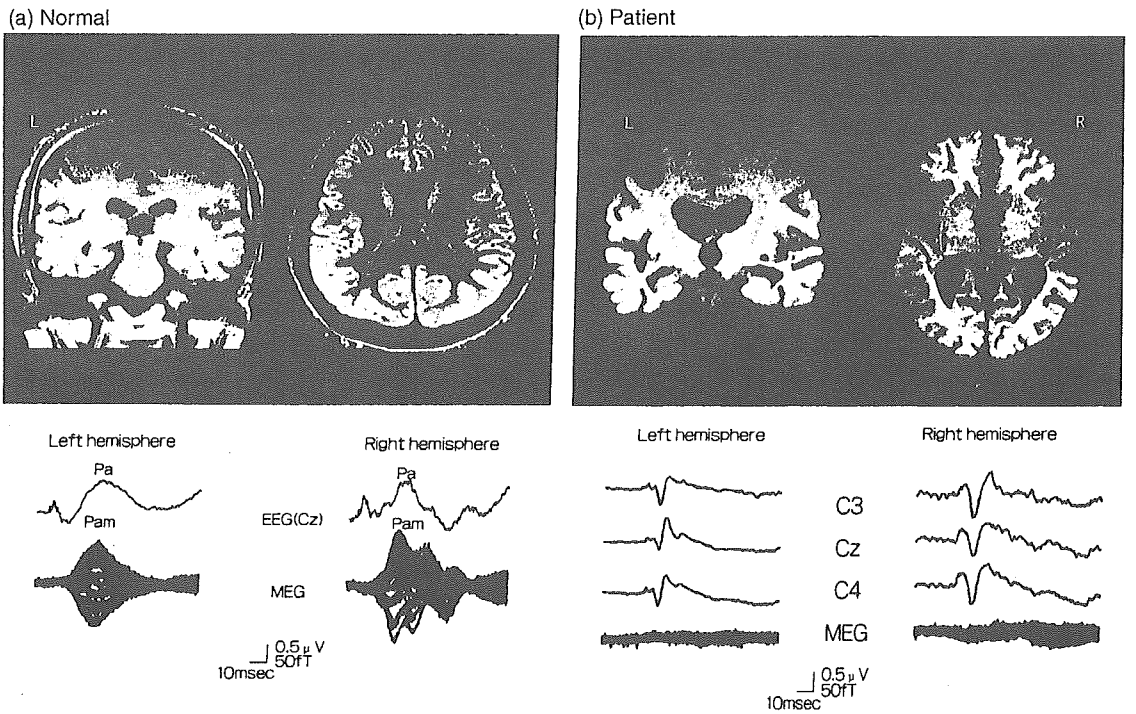

Figure 6. (a) Typical simultaneous recordings of AMLR and MLAEF in a normal subject (25-year-old male). Right and left hemisphere recordings were made with contralateral stimulation. The equivalent current dipole is superimposed on the audiometry cortex in the brain MRI scan. The circle indicates the dipole localization. (b) Simultaneous recordings of AMLR and MLAEF in our patient. The Pam peak in the MLAEF is absent in both hemispheres but a very small Pa peak is present in the AMLR of both hemispheres.

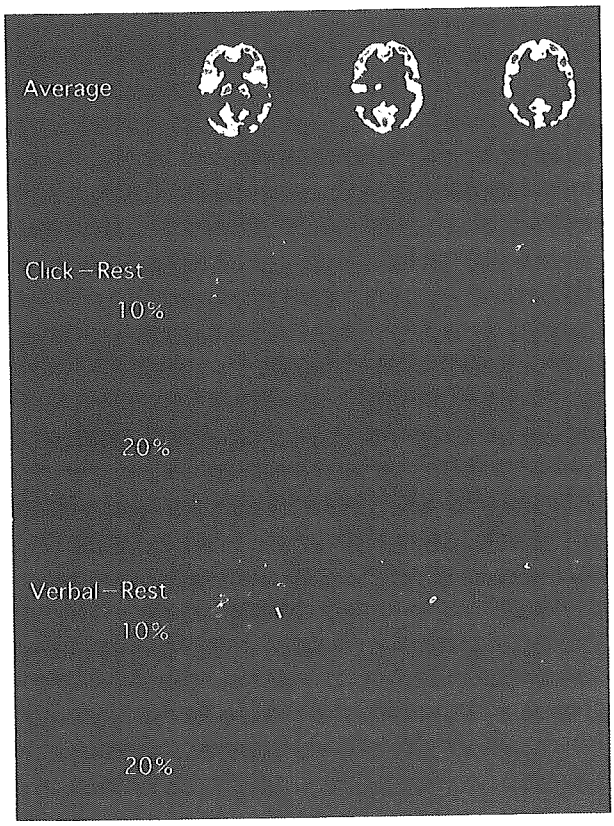

Figure 7. PET scans showing changes in regional cerebral blood flow (CBF) in response to click and verbal stimuli (100 monosyllables). *Top row* = averaged CBF image at rest. *Middle two rows* = increases in CBF over baseline in response to clicks. *Lower two rows* = increases in CBF over baseline in response to verbal stimuli. The images show areas of 10% and 20% increases over baseline blood flow. There are substantial areas showing 10% increases in response to verbal stimuli and smaller areas showing 10% increases in response to clicks. No areas show 20% increases, as would be expected in normal individuals.

the absence of MLAEFs and EMLRs indicated impaired function of the specific auditory pathway as a result of the bilateral lesions of the auditory radiation. In patients with auditory cortex lesions, MLAEFs and EMLRs have been reported to be absent [10]. However, it is significant that our patient could hear but could not discriminate most speech, music and environmental sounds. This discrepancy is considered to be caused by loss of the specific auditory pathway and preservation of the non-specific auditory pathway.

Finally, it is speculated that the auditory cortex receives projections not only from the specific auditory pathway but also from non-specific auditory pathways in the cerebral hemispheres.

Acknowledgement

We thank Ms H. Miyazaki for word processing.

References

[1] Wernicke C, Friedländer C. Ein fall von Taubbeit in folge von doppelsseitiger lesion des Schlä felappens. Fortscshr Med 1883;1:6.

[2] Kaga K, Shindo M, Tanaka Y. Central auditory information processing in patients with bilateral auditory cortex lesions. Acta Otolaryngol Suppl (Stockh) 1997;532:77–82.

[3] Kaga K, Shindo M, Tanaka Y, Haebara H. Neuropathology of auditory agnosia following bilateral temporal lobe lesions. Acta Otolaryngol 2000;120:259–62.

[4] Kaga M, Shindo M, Kaga K. Long-term follow-up of auditory agnosia as a sequel of herpes encephalitis in a child. J Child Neurol 2000;15:626–9.

[5] Rauschecker JP, Tian B. Mechanisms and streams for processing of "what" and "where" in auditory cortex. Proc Natl Acad Sci U S A 2000;97:11800–6.

[6] Pantev C, Lütkenhöner B, Hoke M, Lehnertz K. Comparison between simultaneously measured auditory-evoked magnetic fields and potentials elicited by ipsilateral, contralateral and binaural tone burst stimulation. Audiology 1986;25:54–61.

[7] Pantev C, Hoke M, Lehnertz K, Lütkenhöner B. Neuromagnetic evidence of an amplitopic organization of the human auditory cortex. Electroencephalogr Clin Neurophysiol 1989;72:225–31.

[8] Pelizzone M, Hari R, Mäkelä JP, Huttunen J, Ahlfors S, Hämäläinen M. Cortical origin of middle-latency auditory evoked responses in man. Neurosci Lett 1987;82:303–7.

[9] Mäkelä JP, Hämäläinen M, Hari R, McEvoy L. Whole-head mapping of middle-latency auditory evoked magnetic fields. Electroencephalogr Clin Neurophysiol 1994;92:414–21.

[10] Kaga K, Kurauchi T, Yumoto M, Uno A. Middle-latency auditory evoked magnetic fields in patients with auditory cortex lesions. Acta Otolaryngol 2004;124:376–80.

[11] Kraus N, McGee T, Littsman T, Nicol T. Reticular formation influences on primary and non-primary auditory pathways as reflected by the middle latency response. Brain Res 1992;587:186–94.

[12] Woods DL, Clayworth CC, Knight RT, Simpson GV, Naser MA. Generators of middle- and long-latency auditory evoked potentials: implications from studies of patients with bitemporal lesions. Electroencephalogr Clin Neurophysiol 1987;68:132–48.

DOI:10.1111/j.1365-2125.2005.02514.x

Brain histamine H_1 receptor occupancy of orally administered antihistamines measured by positron emission tomography with ^{11}C-doxepin in a placebo-controlled crossover study design in healthy subjects: a comparison of olopatadine and ketotifen

Manabu Tashiro,[1,3] Hideki Mochizuki,[1] Yumiko Sakurada,[1] Kenji Ishii,[2] Keiichi Oda,[2] Yuichi Kimura,[2] Toru Sasaki,[2] Kiichi Ishiwata[2] & Kazuhiko Yanai[1]

[1]Department of Pharmacology, Tohoku University Graduate School of Medicine, Sendai, Miyagi, Japan; [2]Positron Medical Centre, Tokyo Metropolitan Institute of Gerontology, Tokyo, Japan and [3]Division of Nuclear Medicine, Cyclotron and Radioisotope Centre, Tohoku University, Sendai, Miyagi, Japan

Correspondence
Dr Manabu Tashiro, Division of Nuclear Medicine, Cyclotron and Radioisotope Centre, Tohoku University, 6–3 Aoba, Aramaki, Aoba-ku, Sendai, Miyagi 980–8578, Japan.
Tel: + 81 22 795 7797
Fax: + 81 22 795 7797
E-mail:
mtashiro@mail.tains.tohoku.ac.jp

Keywords
olopatadine, ketotifen, histamine H_1-receptor (H_1R), histamine H_1-receptor occupancy, positron emission tomography (PET), second-generation antihistamine, first-generation antihistamine, placebo-controlled crossover study design

Received
21 May 2004
Accepted
2 August 2005

Aims
The strength of sedation due to antihistamines can be evaluated by using positron emission tomography (PET). The purpose of the present study is to measure histamine H_1 receptor (H_1R) occupancy due to olopatadine, a new second-generation antihistamine and to compare it with that of ketotifen.

Methods
Eight healthy males (mean age 23.5 years-old) were studied following single oral administration of olopatadine 5 mg or ketotifen 1 mg using PET with ^{11}C-doxepin in a placebo-controlled crossover study design. Binding potential ratio and H_1R occupancy were calculated and were compared between olopatadine and ketotifen in the medial prefrontal (MPFC), dorsolateral prefrontal (DLPFC), anterior cingulate (ACC), insular (IC), temporal (TC), parietal (PC), occipital cortices (OC). Plasma drug concentration was measured, and correlation of AUC to H_1R occupancy was examined.

Results
H_1R occupancy after olopatadine treatment was significantly lower than that after ketotifen treatment in the all cortical regions ($P < 0.001$). Mean H_1R occupancies for olopatadine and ketotifen were, respectively: MPFC, 16.7 *vs.* 77.7; DLPFC, 14.1 *vs.* 85.9; ACC, 14.7 *vs.* 76.1; IC, 12.8 *vs.* 69.7; TC, 12.5 *vs.* 66.5; PC, 13.9 *vs.* 65.8; and OC, 19.5 *vs.* 60.6. Overall cortical mean H_1R occupancy of olopatadine and ketotifen were 15% and 72%, respectively. H_1R occupancy of both drugs correlated well with their respective drug plasma concentrations ($P < 0.001$).

Conclusion
It is suggested that 5 mg oral olopatadine, with its low H_1R occupancy and thus minimal sedation, could safely be used an antiallergic treatment for various allergic disorders.

Abbreviations
histamine H_1 receptor (H_1R), histamine H_1 receptor occupancy (H_1RO), dopamine D_2 receptor (D_2R), positron emission tomography (PET), blood–brain barrier (BBB), binding potential ratio (BPR), distribution volume (DV)

Introduction

Histamine H_1 receptor (H_1R) antagonists, or antihistamines, are often used for treatment of allergic disorders such as seasonal rhinitis and conjunctivitis. Antihistamines act mainly on the peripheral system but can induce sedation as a central side-effect. This undesirable side-effect is caused by the blockade of nerve transmission in the histaminergic neurone system, which projects from the nucleus in the posterior hypothalamus to almost all cortical areas [1–3]. First-generation antihistamines, such as ketotifen and d-chlorpheniramine, can easily penetrate the blood–brain barrier, and tend to occupy a large proportion of postsynaptic H_1Rs (>50%) [4–8]. Second-generation antihistamines, such as fexofenadine and terfenadine, are significantly less effective at penetrating the blood–brain barrier and H_1Rs are slightly occupied (<20%) as demonstrated using positron emission tomography (PET) [4, 9]. Variation in cerebral H_1R occupancy (H_1RO) of antihistamines may result from their different permeability through the blood–brain barrier. Thus, the sedative property of antihistamines can be evaluated by the permeability of the blood–brain barrier, measured with PET and [^{11}C]doxepin that can easily penetrate the blood–brain barrier and bind to available H_1Rs in the brain, following administration of the target drug.

Functional neuroimaging techniques such as PET are widely used to evaluate the action and determine minimal effective doses of psychoactive drugs. Indeed, there have been many studies to measure the receptor occupancy of dopaminergic [10–17] and serotonergic [18–22] in schizophrenic and depressive patients. For example, using PET with [^{11}C]raclopride, Nyberg and colleagues demonstrated that the suitable daily dose of risperidone was 4 mg, which achieved sufficiently high dopamine D_2 receptor (D_2R) occupancy of 72%, and that the previous recommended standard dose of 6 mg daily, often accompanied by extrapyramidal side-effects, achieved unnecessarily high D_2R occupancy of 82% [13].

In the case of antihistamines, lower H_1RO in the brain is favoured since they act peripherally. All first-generation antihistamines have sedative properties because of their high blood–brain barrier permeability. However, in the case of second-generation antihistamines, users tend to underestimate their sedative profiles and be less cautious when driving or operating potentially dangerous machinery [1–3]. Moreover, people may take second-generation antihistamines at double or triple doses when recommended doses fail to achieve the desired effects.

Recently, second-generation antihistamines have been further divided into two subgroups. The first includes drugs that cause little sedation at low or recommended doses, but cause dose-related cognitive impairment at higher doses. The other category consists of drugs that do not cross the blood–brain barrier, and thus induce no sedation even at exceeded doses [2, 3]. Thus, it is important to define the sedative threshold for each newly developed drug before launch.

Olopatadine (KW-4679), a new second-generation antihistamine developed in Japan, is widely used as an eye solution for allergic conjunctivitis [23–31] and as an oral treatment for allergic rhinitis and skin diseases [32–35]. Previous studies have compared its efficacy with that of other antiallergic drugs [24–35]. However, only few animal studies [36–38] and one human study [39] have investigated sedative profile of olopatadine. The primary aim of the present study is to measure H_1RO of olopatadine using PET and to compare it with that of ketotifen, a typical sedative antihistamine [40–43], in a placebo-controlled crossover study design. This study design is different from that of our previous studies where control data were obtained from different subjects [4–9].

Methods

The present study was approved by the Committees on Clinical Investigation at both Tohoku University Graduate School of Medicine and Tokyo Metropolitan Institute of Gerontology (TMIG), Japan, and was performed in accordance with the policy of the Declaration of Helsinki. All experiments were performed at the Positron Medical Centre of TMIG.

Subjects and study design

Eight male Japanese subjects (mean age ± SD: 23.9 ± 1.2 years), recruited by advertisement as study-subjects, were given a description of the study, and their written informed consents were obtained. All subjects were in good health with no clinical history of major physical or mental illnesses, showed no abnormality in brain MRI, and were not receiving any concomitant

medication likely to interfere with the study results. Alcohol, nicotine, caffeine, grapefruit and grapefruit juice were forbidden during the study period, and food intake was controlled on the test day and the day before PET measurement. The subjects were requested to finish a light meal by at least 3 h before the study started.

The eight subjects underwent PET measurement after single oral administration of olopatadine 5 mg, ketotifen 1 mg, or a lactobacteria preparation 6 mg used as placebo in a three-way crossover study, with minimum washout intervals of 7 days between treatments. The lactobacteria preparation has been widely used as placebo in Japan, and its administration has resulted in no statistical difference between pre- and postadministration in previous cognitive studies at our department [7, 9, 44]. The present study was single-blinded as the study investigators had to report on each medication, and t_{max} of olopatadine (1.0 ± 0.3 h) was significantly smaller than that of ketotifen (2.8 ± 0.2 h). After drug administration, each subject was asked to lie down in a comfortable position. Blood samples were collected from the subjects before drug administration and at 30, 60, 90, 120 and 150 min postadministration of olopatadine, or at 60, 120, 180, 210 and 240 min postadministration of ketotifen.

Measurement of drug concentrations

Plasma olopatadine and ketotifen concentrations were measured using liquid chromatography/mass spectrometry/mass spectrometry (LC-MS/MS) with an electric spray ionization method. The MS/MS system was an API 4000 (MDS Sciex, Ontario, Canada) in the case of olopatadine or an API 3000 in the case of ketotifen.

For measurement of plasma olopatadine concentration, the Solid Phase Extraction (SPE) cartridge (OASIS HLB, 30 mg/mL, Waters Corporation, Milford, MA, USA) was pretreated with 1 mL of methanol and 1 mL of water. An internal standard solution (150 μL, 250 ng mL^{-1}) and water (150 μL) were added to each plasma sample and the mixture was applied onto the SPE cartridge. LC was performed on a Shimadzu 10 A Vp HPLC instrument (Shimadzu Co., Kyoto, Japan) equipped with an analytical column. Separations were carried out on a C30 reversed-phase HPLC column (Develosil C30-UG-5, Nomura Chemical, Seto, Japan) at a flow rate of 0.2 mL min^{-1}. Detection of olopatadine was based on fragmentation of the precursor ion of m/z = 338 to product ion m/z = 165; the internal standard was based on fragmentation of the precursor ion of m/z = 353 to product ion m/z = 248 under multiple reaction monitoring mode. The lowest detectable concentration was around 0.4 ng mL^{-1} and a coefficient of variation (CV) of olopatadine plasma concentrations measured for quality control ranged from 5.3% to 9.2%. Values below the detectable threshold were extrapolated from the data.

Conditions for measurement of plasma ketotifen concentration were as follows: LC separation was performed on an Agilent 1100 system (Agilent Technologies, Waldbronn, Germany) with a SYNERGI MAX 2.0 × 50 mm (Phenomenex, Torrance, CA, USA) column at a flow rate of 0.25 mL min^{-1}. The reconstituted extract (15 μL) was injected onto an HPLC system with an isocratic mobile phase of 65: 35 v/v 10 mmol L^{-1} ammonium acetate-acetonitrile and a 5.0-min run-time. Positive ions were detected on an API3000 system at a 500 °C nebulizer gas temperature, 3500 V IonSpray voltage, 7 L min^{-1} (air) turbo gas, Concentration 8 (air) nebulizer gas, Concentration 8 (nitrogen) curtain gas and Concentration 10 (nitrogen) collision gas. Ion detection was based on monitoring $[M + H]^+$ ions in the analyte and internal standard in the first quadruple and their corresponding product ions in the third quadruple with a dwell time of 500 ms. Chromatographic data for multiple reaction monitoring (MRM) were collected using Analyst software (version 1.1, AB/MDS SCIEX). The lowest detectable concentration was around 0.1 ng mL^{-1} and a CV of ketotifen concentrations measured for quality control ranged from 0.2% to 5.3%. Values below the detectable threshold were extrapolated from the data.

To examine the relationship between estimated binding potential ratio of [^{11}C]doxepin and plasma concentration of each drug, the area under the curve (AUC) of olopatadine was calculated for 0–150 min ($AUC_{0-2.5\,h}$) postadministration and that of ketotifen for 0–240 min ($AUC_{0-4\,h}$) postadministration.

PET tracer and Image acquisition

[^{11}C]doxepin was prepared by [^{11}C]methylation of desmethyl doxepin with [^{11}C]methyl triflate as described previously [45, 46]. [^{11}C]doxepin radiochemical purity was over 99%, and its specific radioactivity at the time of injection was 58.9 ± 30.1 GBq μmol^{-1} (2719 ± 1113 mCi μmol^{-1}). Saline solution containing [^{11}C]doxepin was intravenously injected into each subject at a time corresponding to t_{max} of each drug (60 min postadministration of olopatadine or 160 min postadministration of ketotifen). The injected dose and cold mass of [^{11}C]doxepin were 259.1 ± 29.5 MBq (7.00 ± 0.80 mCi), and 6.29 ± 5.32 nmol, respectively, and the radiological dose was calculated based on a previous paper on radiological exposure [47]. Blood samples were taken 10 min postinjection of the tracer to measure

radioactivity in the plasma. Labelled metabolites in the plasma were analysed by HPLC as described previously [48]. The percentage of unchanged doxepin was 93.9 ± 3.2 at 10 min postinjection.

Approximately 60 min after [^{11}C]doxepin injection, the subjects were positioned on the coach of the PET scanner (Headtome-V: Shimadzu Co., Kyoto, Japan) so that the transaxial slices were parallel to the orbitomeatal line and a 7-min-long transmission scan was started using ^{68}Ge/^{68}Ga line source for tissue attenuation correction. The subjects were then scanned in order to detect high-energy photon emissions (511 keV) from the [^{11}C]doxepin injected into them. The emission scan was conducted in a three-dimensional (3D) mode, lasting for 15 min (70–85 min postinjection of [^{11}C]doxepin), which acquired 30 slices with 128-by-128 voxels, and at spatial resolutions of 4.5 mm full-width-half-maximum (FWHM) in the transaxial plane and 5.8 mm FWHM in the z-axis [46]. Sensitivity for a 20-cm-long cylindrical phantom was 48.6 kcps kBq^{-1} mL^{-1} (1.8 Mcps μCi^{-1} mL^{-1}) in the 3D mode [49].

PET brain images, after being corrected for tissue attenuation, were reconstructed with a filtered back projection algorithm. The brain images were then normalized by plasma radioactivity at 10 min postinjection to yield static distribution volume images according to our static scan protocol [46, 48]. Our previous investigations confirmed that [^{11}C]doxepin-H_1Rs binding was better described with a two-compartment rather than a three-compartment model, proposing the use of distribution volume as an index of [^{11}C]doxepin binding [46]. We also confirmed that our static scan protocol produced reliable distribution volume values with high correlation efficient ($r = 0.94$) [48].

Three brain images obtained from each subject on different days, following oral administration of olopatadine, ketotifen or placebo, were slightly shifted in x, y and z directions. Using the subject's own MRI-T1 image as a reference, the images were coregistered to the identical stereotaxic brain coordinate system using Statistical Parametric Mapping (SPM99: Welcome Department, UK) software package [50] (Figure 1A). The MRI images were obtained with a SIGNA 1.5 Tesla machine (General Electric Inc., WI, US), TMIG.

Regions of interest (ROIs) were first placed on various brain regions in the MRI-T1 images with precise anatomical information, in the following brain regions: the medial prefrontal (MPFC), dorsolateral prefrontal (DLPFC), anterior cingulate (AC), insular (IC), temporal (TC), parietal (PC), occipital (OC) cortices and on the cerebellum. The ROI information was automatically copied onto the three coregistered distribution volume

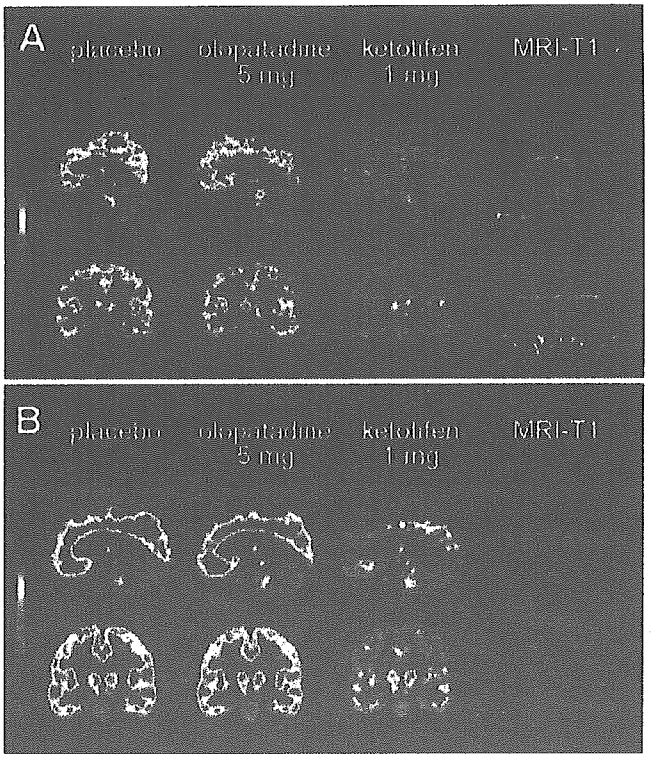

Figure 1
Distribution pattern of ^{11}C-doxepin in the brain of human subjects. Brain distribution volume (DV) of [^{11}C]doxepin was examined in healthy male subjects with PET in three drug conditions, such as placebo (left), olopatadine 5 mg (centre) and ketotifen 1 mg (right) for each subject, as well as their own MRI-T1 image (far right), demonstrated in the sagittal (top) and coronal (bottom) sections for each treatment. (A) Brain DV images of an individual human subject, where the three PET images were coregistered to their own MRI-T1 image as a reference. (B) Mean brain DV images ($n = 8$) averaged from the eight individual brain images following transformation to the standard brain space (spatial normalization). Both demonstrate that ketotifen treatment results in significantly lower DV than the other drug conditions

brain images, and regional distribution volume values were measured in the identical locations in the three drug conditions. Mean voxel values were calculated for the above cortical regions, and binding potential ratio were calculated for each cortical region using the following equation: BPR = [(DV of each region – DV of cerebellum)/DV of cerebellum] [8, 9]. Finally, H_1RO of olopatadine and that of ketotifen were calculated for each cortical region based on the following equation: H_1RO = [(BPR of placebo – BPR with a given antihistamine)/BPR of placebo] × 100 [8, 9, 18, 20].

For visualization at a whole-brain level, distribution volume brain images were statistically analysed on a voxel-by-voxel basis by SPM99, following spatial normalization and smoothing. In spatial normalization,

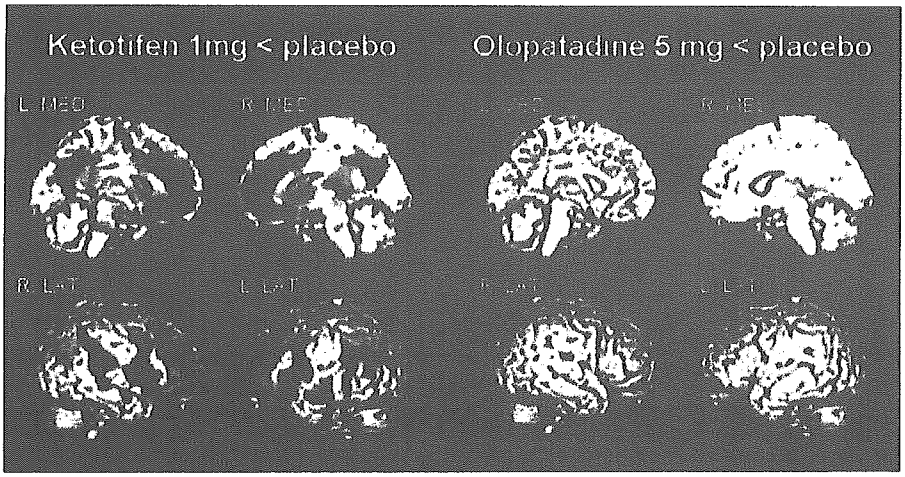

Figure 2
Results of voxel-by-voxel comparison of brain distribution volume (DV) images. The red colour shows areas of significantly lower DV after ketotifen treatment *vs.* after placebo treatment ('Ketotifen 1 mg < placebo' in the left columns). In contrast, there are no areas of significantly lower DV after olopatadine treatment than after placebo treatment ('Olopatadine 5 mg < placebo' in the right columns). In both columns, significant areas are demonstrated in four aspects such as left and right medial (L. MED and R. MED) and right and left lateral (R. LAT and L. LAT) aspects ($P < 0.001$, uncorrected, using SPM99)

Table 1
Plasma concentrations of olopatadine and ketotifen ($n = 8$)

	Olopatadine (ng/ml)				Ketotifen (ng/ml)		
Time (min)	Mean	S.D.	C.V.	Time (min)	Mean	S.D.	C.V.
0	0.0	0.0		0	0.00	0.00	
30	34.0	22.9	**67.4%**	60	0.10	0.05	**50.0%**
60	45.3	13.4	**29.6%**	120	0.23	0.19	**82.6%**
90	39.4	10.7	**27.2%**	180	0.25	0.12	**48.0%**
120	29.4	6.9	**23.5%**	210	0.20	0.13	**65.0%**
150	24.6	6.0	**24.4%**	240	0.17	0.11	**64.7%**
$AUC_{0-2.5\,h}$ [ng/mL*h]	80.2	4.4	**5.5%**	$AUC_{0-4\,h}$ [ng/mL*h]	0.64	0.31	**48.4%**

original distribution volume brain images were transformed to the standard anatomical space to minimize intersubject variation in brain structure [50]. Following the spatial normalization, the images were smoothed by an isotropic Gaussian kernel with FWHM of 12 mm to raise signal : noise (S/N) ratios. Differences in parameter values between olopatadine or ketotifen and placebo (control) were statistically analysed by paired *t*-test (under multisubjects and different conditions), and regional maxima of statistical significance ($P < 0.001$) were projected onto the surface-rendered MRI-T1 standard brain images (Figure 2). Precise locations of the statistically significant regions were identified using Co-Planar Stereotaxic Atlas [51].

Statistical analysis

Differences in binding potential ratio between olopatadine, ketotifen and placebo were examined using ANOVA multiple comparison with Bonferroni correction. The difference in H_1RO between olopatadine and ketotifen was examined using paired Student *t*-test. The relationship between plasma drug concentration and H_1RO value was examined using Pearson's correlation test. A probability of $P < 0.05$ was considered to be statistically significant. All statistical examinations were performed using SPSS for Windows 11.0.1 (Japanese version).

Results

Mean plasma concentrations and AUCs of olopatadine and ketotifen are as shown in Table 1. Mean plasma concentrations of olopatadine and ketotifen reached peak values at 60 min (45.3 ng mL^{-1}) and at 180 min (0.25 ng mL^{-1}) postadministration, respectively, indicating significantly different t_{max} for the two drugs (at 60 min for olopatadine and at 180 min for ketotifen). Large coefficients of variation (CVs) for the plasma

Table 2
Precise information of regions with significant dicrease in specific binding

Regions	Brodmann's area	x, y, z (mm)	Voxel number	T values	Z values	*P* values
Anterior cingulate gyrus	32	0, 34, 26	393	9.46	5.85	<0.001
Fusiform gyrus	20	−42, −20, −38	26	8.76	5.63	<0.001
Medial frontal gyrus	10	−2, 46, −8	189	7.99	5.36	<0.001
Precuneus	31	−2, −62, 28	145	7.99	5.36	<0.001
Posterior cingulate gyrus	31	6, −66, 22		7.12	5.02	<0.001
Middle temporal gyrus	21	−58, −10, −18	17	7.26	5.08	<0.001
Superior temporal gyrus	22	56, 8, 0	28	7.17	5.04	<0.001
Superior temporal gyrus	42	58, −26, 18	37	6.99	4.97	<0.001
Middle frontal gyrus	10	32, 58, 8	23	6.83	4.90	<0.001
Superior frontal gyrus	9	−24, 54, 30	8	6.74	4.87	<0.001
Medial frontal gyrus	10	6, 62, −4	13	6.71	4.85	<0.001

drug concentrations at five measurement points indicated the presence of large intersubject variations in pattern of time-concentration curves, as indicated in Table 1.

$AUC_{0-2.5\,h}$ for olopatadine was 80.2 ng mL^{-1} h^{-1} and its CV was small (5.5%), indicating that there was no large intersubject variation in olopatadine AUC (Table 1). $AUC_{0-4\,h}$ for ketotifen was 0.64 ng mL^{-1} h^{-1} with a large CV (48.4%), indicating that the intersubject variability for ketotifen AUC was large, possibly due to the low plasma ketotifen concentrations near to the detectable threshold (Table 1).

The radioactivity distribution pattern of [^{11}C]doxepin is shown in Figure 1. The distribution volume brain image following treatment with olopatadine was similar to that following treatment with placebo in an individual subject (Figure 1A). The same trend was consistently observed in the averaged distribution volume brain image, based on the spatially normalized brain images of the eight subjects (Figure 1B), representing the mean radioactivity distribution pattern. High radioactivity was observed in the MPFC, DLPFC, ACC, IC, TC, PC, OC, and thalamus following treatment with olopatadine and placebo (Figure 1). In contrast, the radioactivity distribution pattern following treatment with ketotifen was much lower than that following the treatment with olopatadine or placebo.

Using SPM99 on a voxel-by-voxel basis, parametric brain distribution volume images following treatment with olopatadine or ketotifen were statistically compared with those following treatment with placebo. In Figure 2, the red areas show brain regions where distribution volumes were significantly lower ($P < 0.001$) following treatment with ketotifen than following treatment with placebo (Figure 2, left). Areas such as ACC, MPFC, DLPFC, and TC demonstrated significantly low distribution volumes after treatment with ketotifen compared with placebo (Table 2). Conversely, SPM analysis did not reveal any brain area where distribution volumes were significantly lower following treatment with olopatadine compared with placebo (Figure 2, right).

Binding potential ratio values in H_1R-rich regions such as MPFC, DLPFC, ACC, IC, TC, PC and OC were evaluated based on ROI analysis (Figure 3A). Binding potential ratio values following treatment with olopatadine were only slightly different from those following treatment with placebo. However, binding potential ratio values following treatment with ketotifen were significantly lower than those following treatment with placebo or olopatadine ($P < 0.001$ for all regions studied) with the following 95% CI values for mean binding potential ratio differences from placebo: MPFC, 0.25, 0.54; DLPFC, 0.25, 0.47; ACC, 0.35, 0.64; IC, 0.28, 0.55; TC, 0.22, 0.52; PC, 0.24, 0.50; and OC, 0.17, 0.37; and from olopatadine: MPFC, 0.16, 0.45; DLPFC, 0.19, 0.41; ACC, 0.25, 0.54; IC, 0.20, 0.47; TC, 0.15, 0.45; PC, 0.16, 0.43; and OC, 0.08, 0.28.

H_1RO values following treatment with olopatadine or ketotifen were also calculated using the value of H_1RO following treatment with placebo as baseline (0%) (Figure 3B). Mean H_1RO following treatment with olopatadine was approximately 15% (mean H_1RO ± SD MPFC, 16.7 ± 10.0; DLPFC, 14.1 ± 9.6; ACC, 14.7 ± 9.1; IC, 12.8 ± 7.9; TC, 12.5 ± 7.1; PC, 13.9 ± 5.6; and OC, 19.5 ± 10.6) and that following treatment with ketotifen was approximately 72% (mean H_1RO ± SD MPFC, 77.7 ± 10.3; DLPFC, 85.9 ± 12.2; ACC, 76.1 ± 9.5; IC,

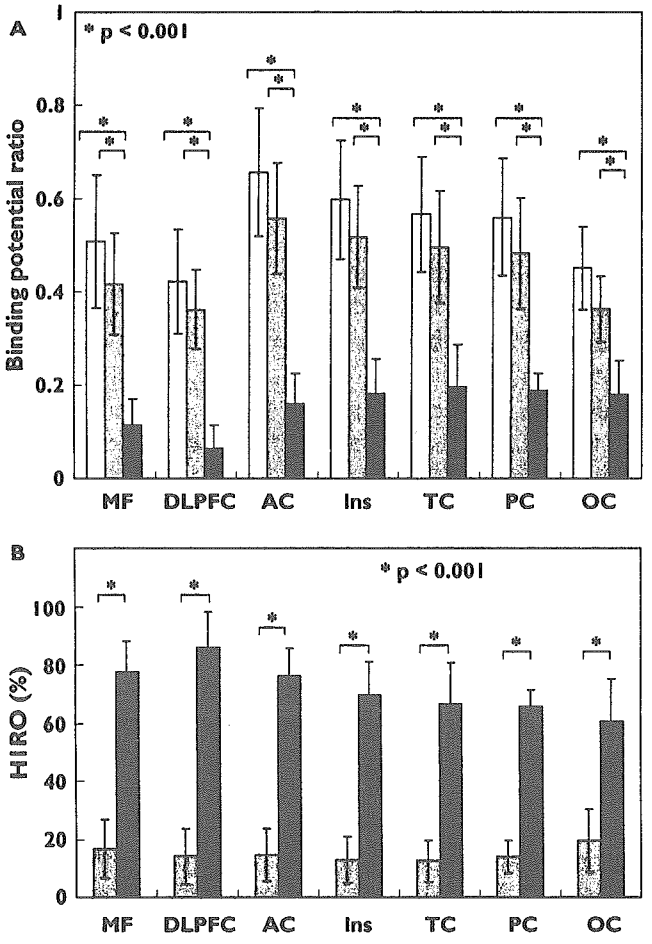

Figure 3

Region of interest (ROI)-based analyses of (A)binding potential ratios (BPR) and (B) histamine H_1 receptor occupancy (H_1RO) in the cortex. ROI measurements were taken in the medial prefrontal (MPFC), dorsolateral prefrontal (DLPFC), anterior cingulate (AC), insular (IC), temporal (TC), parietal (PC), occipital cortex (OC) after treatment with antihistamines. Comparison of BPRs shows differences in the sedative properties of the three drugs such as placebo (PLA), olopatadine (OLO) and ketotifen (KET) (A). H_1RO by the two antihistamines are shown taking H_1RO by the placebo as 0% (B). $P < 0.001$, statistically examined by ANOVA followed by multiple comparison by Bonferroni test. The error bars represent interindividual variability (SD). PLA (□); OLO (▨); KET (■)

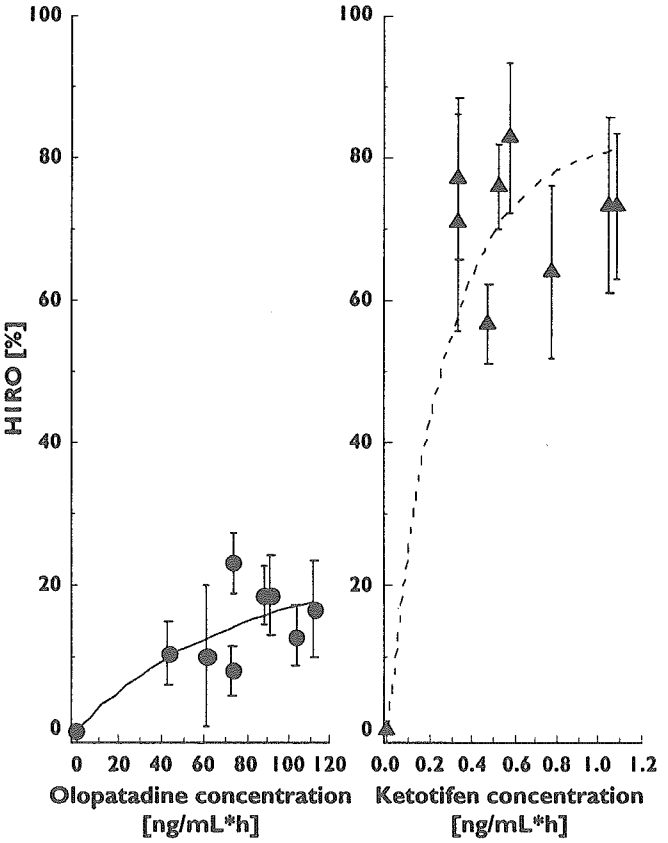

Figure 4

Relationship between mean H_1RO and olopatadine (left) and ketotifen plasma concentrations (right). Plasma concentrations of the two antihistamines are presented as area under the curve (AUC). Correlation efficients examined by Pearson's correlation test were 0.76 for olopatadine ($P < 0.001$) and 0.86 for ketotifen ($P < 0.001$). H_1RO of ketotifen rises rapidly with increments in plasma concentration whereas H_1RO of olopatadine rises slowly with increments in plasma concentration. The error bars represent intraindividual variability (SEM)

69.7 ± 11.3; TC, 66.5 ± 14.2; PC, 65.8 ± 5.5; and OC, 60.6 ± 14.6). H_1RO values following treatment with olopatadine were significantly lower than those following treatment with ketotifen ($P < 0.001$) for all cortical regions studied with the following mean binding potential ratio differences (95% CI) between olopatadine and ketotifen: MPFC, 51.8, 70.2; DLPFC, 59.8, 83.7; TC, 40.1, 58.5; PC, 38.5, 54.7; OC, 26.6, 48.2; ACC, 50.7, 72.2; IC, 42.3, 60.8. These data demonstrate that binding potential ratio following treatment with olopatadine is substantially higher than that following treatment with ketotifen in all cortical regions studied.

Correlations between H_1ROs and AUCs of olopatadine and ketotifen concentrations were examined across the subjects. The H_1ROs correlated well to the AUCs with the correlation coefficients of 0.83 for both drug conditions (Pearson's test, $P < 0.001$). H_1RO of olopatadine rose slowly with increment in olopatadine $AUC_{0-2.5\,h}$. H_1RO of ketotifen tended to rise rapidly with increment in ketotifen $AUC_{0-4\,h}$ (Figure 4). Although the CV of ketotifen $AUC_{0-4\,h}$ was high, possibly because ketotifen concentrations took very low values near to the detectable threshold, the result of significant correlation between ketotifen $AUC_{0-4\,h}$ and H_1RO was in accordance with the results of previous studies on other sedative antihistamines such as d-chlorpheniramine [7, 8].

Discussion

Recently, noninvasive *in vivo* measurement of neuroreceptor occupancy has been conducted in humans for the development of various psychoactive drugs [10–22]. In the present study, H_1RO of olopatadine, a second-generation antihistamine, was compared with that of ketotifen, a typical sedative antihistamine, in a single-blinded placebo-controlled crossover study design.

H_1RO after a single oral administration of olopatadine 5 mg or ketotifen 1 mg was calculated as approximately 15% and 72%, respectively. The high value for ketotifen corresponds with the H_1RO value reported in a previous clinical trial (76.8%, $n = 3$) where the averaged baseline value ($n = 6$) was obtained from different subjects [6]. It has also been reported that, single-oral administration of d-chlorpheniramine (2 mg) achieved approximately 50–77% of H_1RO [4, 8]. In addition, brain H_1RO due to d-chlorpheniramine seems to increase rapidly in a concentration-dependent manner [7, 8] in a similar fashion to that due to ketotifen in the present study, although the large CV value of ketotifen $AUC_{0-4\,h}$ would limit the reliability of the correlation analysis (Figure 4). Previous PET studies demonstrated that first-generation antihistamines occupied more than 50% of available H_1Rs. This high H_1RO is associated with high prevalence of sleepiness and cognitive decline [5, 8].

Conversely, H_1RO after single-oral administration of olopatadine (5 mg) was much lower than that of first-generation antihistamines (15% *vs.* >50%). This result corresponds with the categorization of olopatadine as a second-generation antihistamine. Previous studies have demonstrated H_1RO values due to other second-generation antihistamines: epinastine 20 mg (8.2–13.2%) [5, 6], terfenadine 60 mg (12.1–17.1%) [4, 6], astemizole 10 mg (28.7%), azelastine 1 mg (20.3%), mequitazine 3 mg (22.2%) [6] and ebastine 10 mg (9.9%) [8]. Second-generation antihistamines occupy around 0–20% of brain H_1Rs [6]. Single-oral doses of cetirizine 20 mg and fexofenadine 120 mg, both double oral doses in Japan, have been reported to achieve 26% and 0%, respectively [9]. Based on such findings, second-generation antihistamines can be further separated into two subgroups according to their blood–brain barrier permeabilities [2, 3]; one category that causes little sedation at low doses, but causes dose-related cognitive impairment at higher doses, as seen with cetirizine; the other category that does not cross the blood–brain barrier and therefore induces no sedation even at exceeded doses, as seen with fexofenadine [9].

Such variation in blood–brain barrier permeability among antihistamines has been explained by various factors such as different lipophilicity, molecular size and different actions of drug transporters. Lipophilic antihistamines, as seen with many first-generation antihistamines, can be absorbed in a full amount in the gut, and can freely penetrate the blood–brain barrier. In the case of second-generation antihistamines, with decreased lipophilicity, absorption in the gut would be limited. P-glycoprotein, an efflux pump expressed in the blood–brain barrier, gut barrier and in other organs, may be playing the most important role in blood–brain barrier permeability [52]. In the case of fexofenadine, a known substrate of P-gp, both gut absorption and blood–brain barrier permeability would decrease further. In the blood–brain barrier particularly, there is a strict barrier with tight junctions between capillary endothelial cells and with astroglial processes, where few fexofenadine molecules can penetrate and enter the brain. Whether olopatadine is a substrate of P-gp is currently under investigation.

The socially important detail is that although some second-generation antihistamines appear to be nonsedative, they are mildly sedative with increased doses. Based on these findings, a recent expert meeting (the Consensus Group on New Generation Antihistamines: CONGA) states that H_1RO measured by PET should be under 20% at the highest recommended dose [2]. From this standpoint, olopatadine seems to belong to the same category as cetirizine, as its brain H_1RO seems to increase in a concentration-dependent manner as demonstrated in Figure 4. This assumption corresponds with a recent human study demonstrating that olopatadine 10 mg (a double oral dose in Japan) induced mild psychomotor impairment among healthy subjects [39]. In addition, animal studies may provide further suggestions [33, 36–38]. No EEG changes were observed after oral administration of olopatadine in rabbits [33] and in rats [36], whereas oral ketotifen induced significant sedation in both animal studies [33, 36]. Another rat study demonstrated that 10 mg kg^{-1} oral administration of olopatadine did not affect behaviour in rats whereas 50 mg kg^{-1} oral administration of olopatadine induced significant sedation [37]. It is assumed that the therapeutic dose of olopatadine (single oral dose at 5 mg) is reasonably safe and suitable in terms of avoiding sedative side-effects. The final conclusions regarding the sedative effects of single oral administration of olopatadine 5 mg should be drawn combined with the results of a planned double-blinded placebo-controlled study on psychomotor performance and subjective sleepiness.

The present study succeeded in demonstrating sedation due to antihistamines in healthy subjects, but it does not describe subjective sedation owing to other origins, as seen in allergic patients even at preadministration of

antihistamines and relieved postadministration [53]. Other causes for such subjective sedation would be the contribution of other chemical mediators (prostaglandins, etc) and mental and physical factors due to irritating symptoms such as nasal plugging and sand eyes. The authors do not yet know the extent to which such factors would affect PET results of a similar study conducted in patients with active allergy.

This is the first PET study on antihistamines, following a placebo-controlled crossover study design where we were able to minimize potential errors due to inter-subject variability. This is probably the most important advantage of our study design, which makes interpretation of results easier and clearer. To our knowledge, placebo-controlled crossover study design was first used with PET to investigate dopamine D_1 or D_2 receptor occupancies by new antagonists such as NNC 756 [10], sertindole [12] and risperidone [13]. Only two complete placebo-controlled crossover studies [18, 21] and a few partially crossover studies regarding serotonin receptors (5HT1A receptors) were available [19, 22]. Compared with PET studies in a clinical trial design, the number of complete placebo-controlled PET studies is generally limited [11, 14–17, 54].

Placebo-controlled crossover studies are disadvantaged by the increased radiological exposure, as each subject is scanned more than twice. Investigators are therefore advised to minimize total radiation exposure to subjects by choosing a minimum radiological dose and by using 3D data acquisition mode with high sensitivity. In addition, mental and physical stress of the subjects should be decreased by simplifying measurement protocol, as in the present study where complete datasets were obtained for all of the eight subjects. In a study by Martinez *et al.* [18] only 6 of the 11 subjects completed all four 100-min-long PET scans planned, which reflects the difficulty of conducting crossover PET studies.

In summary, we examined H_1RO of olopatadine at its highest recommended single oral dose (5 mg) and compared it with that of single oral administration of ketotifen (1 mg) using PET measurement in a placebo-controlled crossover study. Olopatadine occupied approximately 15% of available H_1Rs in the human brain whereas approximately 72% of H_1Rs were occupied by 1 mg of ketotifen. It is therefore suggested that oral administration of olopatadine (5 mg), with its low H_1RO and thus minimal sedation, could safely be used an antiallergic treatment for various allergic disorders.

It would be of a great aid in estimating the appropriate therapeutic doses of new antihistamines and other drugs using PET measurement and the minimum number of subjects (6 to 10 subjects). Collection of more H_1RO data is encouraged for establishment of a reliable international database for evaluation of the sedative profile of antihistamines.

This work was in part supported by Grants-in-Aid for scientific research (No. 12557007, 14370027, 14770489) from the Japan Society of Promotion of Science (JSPS) and a 21st Century COE program (Bio-nano-technology) from the Ministry of Education, Culture, Sports, Science and Technology, Japan. This work was also supported by Sagawa Traffic Safety Foundation (to Tashiro M). The authors thank the subjects in the PET measurement, Ms Miyoko Ando for care of subjects and Dr Kazunori Kawamura for the preparation of [^{11}C]doxepin.

References

1 Haas H, Panula P. The role of histamine and the tuberomamillary nucleus in the nervous system. Nat Rev Neurosci 2003; 4 (2): 121–30.

2 Holgate ST, Canonica GW, Simons FE, Taglialatela M, Tharp M, Timmerman H, Yanai K. Consensus Group on New-Generation Antihistamines (CONGA): present status and recommendations. Clin Exp Allergy 2003; 33 (9): 1305–24.

3 Casale TB, Blaiss MS, Gelfand E, Gilmore T, Harvey PD, Hindmarch I, Simons FE, Spangler DL, Szefler SJ, Terndrup TE, Waldman SA, Weiler J, Wong DF. First do no harm: managing antihistamine impairment in patients with allergic rhinitis. J Allergy Clin Immunol 2003; 111 (5): S835–42.

4 Yanai K, Ryu JH, Watanabe T, Iwata R, Ido T, Sawai Y, Ito K, Itoh M. Histamine H1 receptor occupancy in human brains after single oral doses of histamine H1 antagonists measured by positron emission tomography. Br J Pharmacol 1995; 116 (1): 1649–55.

5 Yanai K, Ryu JH, Watanabe T, Iwata R, Ido T, Asakura M, Matsumura R, Itoh M. Positron emission tomographic study of central histamine H1-receptor occupancy in human subjects treated with epinastine, a second-generation antihistamine. Meth Find Exp Clin Pharmacol 1995; 17(Suppl C): 64–9.

6 Yanai K, Okamura N, Tagawa M, Itoh M, Watanabe T. New findings in pharmacological effects induced by antihistamines: from PET studies to knock-out mice. Clin Exp Allergy 1999; 29(Suppl 3): 29–36; discussion 37–8.

7 Okamura N, Yanai K, Higuchi M, Sakai J, Iwata R, Ido T, Sasaki H, Watanabe T, Itoh M. Functional neuroimaging of cognition impaired by a classical antihistamine, d-chlorpheniramine. Br J Pharmacol 2000; 129 (1): 115–23.

8 Tagawa M, Kano M, Okamura N, Higuchi M, Matsuda M, Mizuki Y, Arai H, Iwata R, Fujii T, Komemushi S, Ido T, Itoh M, Sasaki H, Watanabe T, Yanai K. Neuroimaging of histamine H1-receptor occupancy in human brain by positron emission tomography

(PET): a comparative study of ebastine, a second-generation antihistamine, and (+)- chlorpheniramine, a classical antihistamine. Br J Clin Pharmacol 2001; 52 (5): 501–9.

9 Tashiro M, Sakurada Y, Iwabuchi K, Mochizuki H, Kato M, Aoki M, Funaki Y, Itoh M, Iwata R, Wong DF, Yanai K. Central effects of fexofenadine and cetirizine. Measurement of psychomotor performance, subjective sleepiness, and brain histamine H1-receptor occupancy using ^{11}C-doxepin positron emission tomography. J Clin Pharmacol 2004; 44 (8): 890–900.

10 Karlsson P, Farde L, Halldin C, Sedvall G, Ynddal L, Sloth-Nielsen M. Oral administration of NNC 756 – a placebo controlled PET study of D1-dopamine receptor occupancy and pharmacodynamics in man. Psychopharmacology (Berl) 1995; 119 (1): 1–8.

11 de Haan L, van Bruggen M, Lavalaye J, Booij J, Dingemans PM, Linszen D. Subjective experience and D_2 receptor occupancy in patients with recent-onset schizophrenia treated with low-dose olanzapine or haloperidol: a randomized, double-blind study. Am J Psychiatry 2003; 160 (2): 303–9.

12 Nyberg S, Olsson H, Nilsson U, Maehlum E, Halldin C, Farde L. Low striatal and extra-striatal D_2 receptor occupancy during treatment with the atypical antipsychotic sertindole. Psychopharmacology (Berl) 2002; 162 (1): 37–41.

13 Nyberg S, Eriksson B, Oxenstierna G, Halldin C, Farde L. Suggested minimal effective dose of risperidone based on PET-measured D_2 and 5-HT2A receptor occupancy in schizophrenic patients. Am J Psychiatry 1999; 156 (6): 869–75.

14 Bernardo M, Parellada E, Lomena F, Catafau AM, Font M, Gomez JC, Lopez-Carrero C, Gutierrez F, Pavia J, Salamero M. Double-blind olanzapine vs. haloperidol D_2 dopamine receptor blockade in schizophrenic patients: a baseline-endpoint. Psychiatry Res 2001; 107 (2): 87–97.

15 Kapur S, Zipursky R, Jones C, Remington G, Houle S. Relationship between dopamine D(2) occupancy, clinical response, and side effects: a double-blind PET study of first-episode schizophrenia. Am J Psychiatry 2000; 157 (4): 514–20.

16 Martinot JL, Paillere-Martinot ML, Poirier MF, Dao-Castellana MH, Loc'h C, Maziere B. In vivo characteristics of dopamine D_2 receptor occupancy by amisulpride in schizophrenia. Psychopharmacology (Berl) 1996; 124 (1–2): 154–8.

17 Nordstrom AL, Farde L, Wiesel FA, Forslund K, Pauli S, Halldin C, Uppfeldt G. Central D_2-dopamine receptor occupancy in relation to antipsychotic drug effects: a double-blind PET study of schizophrenic patients. Biol Psychiatry 1993; 33 (4): 227–35.

18 Martinez D, Hwang D, Mawlawi O, Slifstein M, Kent J, Simpson N, Parsey RV, Hashimoto T, Huang Y, Shinn A, Van Heertum R, Abi-Dargham A, Caltabiano S, Malizia A, Cowley H, Mann JJ, Laruelle M. Differential occupancy of somatodendritic and postsynaptic 5HT (1A) receptors by pindolol: a dose-occupancy study with [^{11}C]WAY 100635 and positron emission tomography in humans. Neuropsychopharmacology 2001; 24 (3): 209–29.

19 Rabiner EA, Bhagwagar Z, Gunn RN, Sargent PA, Bench CJ, Cowen PJ, Grasby PM. Pindolol augmentation of selective serotonin reuptake inhibitors: PET evidence that the dose used in clinical trials is too low. Am J Psychiatry 2001; 158 (12): 2080–2.

20 Rabiner EA, Wilkins MR, Turkheimer F, Gunn RN, de Haes JU, de Vries M, Grasby PM. 5-Hydroxytryptamine1A receptor occupancy by novel full antagonist 2-[4-[4-(7-chloro-2,3-dihydro-1,4-benzdioxyn-5-yl) -1-piperazinyl]butyl]-1, 2-benzisothiazol-3-(2H) -one-1,1-dioxide: a[^{11}C][O-methyl-3H]-N-(2-(4-(2-methoxyphenyl) -1-piperazinyl) ethyl) -N-(2-py ridinyl) cyclohexanecarboxamide trihydrochloride (WAY-100635) positron emission tomography study in humans. J Pharmacol Exp Ther 2002; 301 (3): 1144–50.

21 Nakayama T, Suhara T, Okubo Y, Ichimiya T, Yasuno F, Maeda J, Takano A, Saijo T, Suzuki K. In vivo drug action of tandospirone at 5-HT1A receptor examined using positron emission tomography and neuroendocrine response. Psychopharmacology (Berl) 2002; 165 (1): 37–42.

22 Andree B, Nyberg S, Ito H, Ginovart N, Brunner F, Jaquet F, Halldin C, Farde L. Positron emission tomographic analysis of dose-dependent MDL 100, 907 binding to 5–hydroxytryptamine–2A receptors in the human brain. J Clin Psychopharmacol 1998; 18 (4): 317–23.

23 Abelson MB, Spitalny L. Combined analysis of two studies using the conjunctival allergen challenge model to evaluate olopatadine hydrochloride, a new ophthalmic antiallergic agent with dual activity. Am J Ophthalmol 1998; 125 (6): 797–804.

24 Katelaris CH, Ciprandi G, Missotten L, Turner FD, Bertin D, Berdeaux G. A comparison of the efficacy and tolerability of olopatadine hydrochloride 0.1% ophthalmic solution and cromolyn sodium 2% ophthalmic solution in seasonal allergic conjunctivitis. Clin Ther 2002; 24 (10): 1561–75.

25 Spangler DL, Bensch G, Berdy GJ. Evaluation of the efficacy of olopatadine hydrochloride 0.1% ophthalmic solution and azelastine hydrochloride 0.05% ophthalmic solution in the conjunctival allergen challenge model. Clin Ther 2001; 23 (8): 1272–80.

26 Berdy GJ, Spangler DL, Bensch G, Berdy SS, Brusatti RC. A comparison of the relative efficacy and clinical performance of olopatadine hydrochloride 0.1% ophthalmic solution and ketotifen fumarate 0.025% ophthalmic solution in the conjunctival antigen challenge model. Clin Ther 2000; 22 (7): 826–33.

27 Artal MN, Luna JD, Discepola M. A forced choice comfort study of olopatadine hydrochloride 0.1% versus ketotifen fumarate 0.05%. Acta Ophthalmol Scand Suppl 2000; 230: 64–5.

28 Aguilar AJ. Comparative study of clinical efficacy and tolerance in seasonal allergic conjunctivitis management with 0.1% olopatadine hydrochloride versus 0.05% ketotifen fumarate. Acta Ophthalmol Scand Suppl 2000; 230: 52–5.

29 Butrus S, Greiner JV, Discepola M, Finegold I. Comparison of the clinical efficacy and comfort of olopatadine hydrochloride 0.1% ophthalmic solution and nedocromil sodium 2% ophthalmic solution in the human conjunctival allergen challenge model. Clin Ther 2000; 22 (12): 1462–72.

30 Abelson MB, Welch DL. An evaluation of onset and duration of action of patanol (olopatadine hydrochloride ophthalmic solution 0.1%) compared to Claritin (loratadine 10 mg) tablets in acute allergic conjunctivitis in the conjunctival allergen challenge model. Acta Ophthalmol Scand Suppl 2000; 230: 60–3.

31 Yanni JM, Weimer LK, Sharif NA, Xu SX, Gamache DA, Spellman JM. Inhibition of histamine-induced human conjunctival epithelial cell responses by ocular allergy drugs. Arch Ophthalmol 1999; 117 (5): 643–7.

32 Ohmori K, Hayashi K, Kaise T, Ohshima E, Kobayashi S, Yamazaki T, Mukouyama A. Pharmacological pharmacokinetic and clinical properties of olopatadine hydrochloride, a new antiallergic drug. Jpn J Pharmacol 2002; 88 (4): 379–97.

33 Ishii H, Sasaki Y, Manabe H, Ikemura T, Sato H, Ichikawa S, Shiozaki S, Kitamura S, Ohmori K. [General pharmacology of KW-4679, an antiallergic drug (1st report): effects on central nervous system, autonomic nervous system and peripheral nervous system]. Clin Pharmacol Ther 1995; 5 (8): 1421–40. in Japanese.

34 Hamilton SA, Duddle J, Herdman MJ, Trigg CJ, Davies RJ. Comparison of a new antihistaminic and antiallergic compound KW 4679 with terfenadine and placebo on skin and nasal provocation in atopic individuals. Clin Exp Allergy 1994; 24 (10): 955–9.

35 Morita K, Koga T, Moroi Y, Urabe K, Furue M. Rapid effects of olopatadine hydrochloride on the histamine-induced skin responses. J Dermatol 2002; 29 (11): 709–12.

36 Kamei C, Ichiki C, Izumo T, Ohishi H, Yoshida T, Tsujimoto S. Effect of the new antiallergic agent olopatadine on EEG spectral powers in conscious rats. Arzneimittelforschung 1996; 46 (8): 789–93.

37 Kamei C, Nishiga M, Shigemoto Y, Konishi M, Shinomiya K. [Effect of epinastine hydrochloride (Alesion) on the central nervous system.] Jpn Pharmacol Ther 2002; 30 (2): 91–5.

38 Nishiga M, Fujii Y, Konishi M, Hossen MA. Effects of second-generation histamine H1 receptor antagonists on the active avoidance response in rats. Clin Exp Pharmacol Physiol 2003; 30 (1–2): 60–3.

39 Kamei H, Noda Y, Ishikawa K, Senzaki K, Muraoka I, Hasegawa Y, Hindmarch I, Nabeshima T. Comparative study of acute effects of single doses of fexofenadine, olopatadine, d-chlorpheniramine and placebo on psychomotor function in healthy volunteers. Hum Psychopharmacol 2003; 18 (8): 611–8.

40 Grant SM, Goa KL, Fitton A, Sorkin EM. Ketotifen. A review of its pharmacodynamic and pharmacokinetic properties, and therapeutic use in asthma and allergic disorders. Drugs 1990; 40 (3): 412–48.

41 Simons FE, Fraser TG, Reggin JD, Simons KJ. Comparison of the central nervous system effects produced by six H1-receptor antagonists. Clin Exp Allergy 1996; 26 (9): 1092–7.

42 Matejcek M, Irwin P, Neff G, Abt K, Wehrli W. Determination of the central effects of the asthma prophylactic ketotifen, the bronchodilator theophylline, and both in combination: an application of quantitative electroencephalography to the study of drug interactions. Int J Clin Pharmacol Ther Toxicol 1985; 23 (5): 258–66.

43 Vollmer R, Matejcek M, Greenwood C, Grisold W, Jellinger K. Correlation between EEG changes indicative of sedation and subjective responses. Neuropsychobiology 1983; 10 (4): 249–53.

44 Tagawa M, Kano M, Okamura N, Higuchi M, Matsuda M, Mizuki Y, Arai H, Fujii T, Komemushi S, Itoh M, Sasaki H, Watanabe T, Yanai K. Differential cognitive effects of ebastine and (+) -chlorpheniramine in healthy subjects: correlation between cognitive impairment and plasma drug concentration. Br J Clin Pharmacol 2002; 53 (3): 296–304.

45 Iwata R, Pascali C, Bogni A, Miyake Y, Yanai K, Ido T. A simple loop method for the automated preparation of (^{11}C) raclopride from (^{11}C) methyl triflate. Appl Radiat Isot 2001; 55 (1): 17–22.

46 Mochizuki H, Kimura Y, Ishii K, Oda K, Sasaki T, Tashiro M, Yanai K, Ishiwata K. Quantitative measurement of histamine H (1) receptors in human brains by PET and [^{11}C]doxepin. Nucl Med Biol 2004; 31 (2): 165–71.

47 Nakamura T, Hayashi Y, Watabe H, Matsumoto M, Horikawa T, Fujiwara T, Ito M, Yanai K. Estimation of organ cumulated activities and absorbed doses on intakes of several ^{11}C labelled radiopharmaceuticals from external measurement with thermoluminescent dosimeters. Phys Med Biol 1998; 43 (2): 389–405.

48 Mochizuki H, Kimura Y, Ishii K, Oda K, Sasaki T, Tashiro M, Yanai K, Ishiwata K. Simplified PET measurement for evaluating histamine H1 receptors in human brains using [^{11}C]doxepin. Nucl Med Biol 2004; 31 (8): 1005–11.

49 Fujiwara T, Watanuki S, Yamamoto S, Miyake M, Seo S, Itoh M, Ishii K, Orihara H, Fukuda H, Satoh T, Kitamura K, Tanaka K, Takahashi S. Performance evaluation of a large axial field-of-view PET scanner SET-2400w. Ann Nucl Med 1997; 11 (4): 307–13.

50 Friston KJ, Holmes AP, Worsley KJ, Poline JP, Frith CD, Frackowiak RSJ. Statistical parametric maps in functional imaging: a general linear approach. Hum Brain Mapp 1995; 2: 189–210.

51 Talairach J, Tournoux P. Co-Planar Stereotaxic Atlas of the Human Brain. Stuttgart. Germany: Georg Thieme Verlag, 1988.

52 Drescher S, Schaeffeler E, Hitzl M, Hofmann U, Schwab M, Brinkmann U, Eichelbaum M, Fromm MF. MDR1 gene polymorphisms and disposition of the P-glycoprotein substrate fexofenadine. Br J Clin Pharmacol 2002; 53 (5): 526–34.

53 Spaeth J, Klimek L, Mosges R. Sedation in allergic rhinitis is caused by the condition and not by antihistamine treatment. Allergy 1996; 51 (12): 893–906.

54 Bench CJ, Lammertsma AA, Dolan RJ, Grasby PM, Warrington SJ, Gunn K, Cuddigan M, Turton DJ, Osman S, Frackowiak RS. Dose dependent occupancy of central dopamine D_2 receptors by the novel neuroleptic CP-88,059–01: a study using positron emission tomography and ^{11}C-raclopride. Psychopharmacology (Berl) 1993; 112 (2–3): 308–14.